

# Fracture and fatigue of discontinuously reinforced copper/tungsten composites

B. HARRIS, S. V. RAMANI\*

*School of Applied Sciences, University of Sussex, Brighton, UK*

The strength, toughness and resistance to cyclic crack propagation of composites consisting of copper reinforced with short tungsten wires of various lengths have been studied and the results compared with the behaviour of continuously reinforced composites manufactured by the same method, i.e. by vacuum hot-pressing. It has been found that whereas the resistance to fatigue crack growth of continuously reinforced composites is very similar to that of continuous Al/stainless steel composites reported elsewhere, the addition of short fibres completely changes the mode of fracture, and no direct comparisons are possible. In effect, short fibres inhibit single crack growth by causing plastic flow to be distributed rather than localized, and although these composites are much less strong than continuous fibre composites, they nevertheless have much greater fatigue resistance. The fracture toughness of the composites is thought to be derived simply from the separate contributions of matrix and fibre plastic flow and, in composites containing fibres near to the critical length, from the very substantial work of fibre pull-out.

## 1. Introduction

In a study of fatigue and fracture of an aluminium alloy reinforced with continuous tungsten wires, McGuire and Harris [1] attempted to show the effect of matrix work-hardening behaviour on crack propagation in these composites. They concluded that the effect of differences in the plastic deformation characteristics of the matrix alloy was insignificant at fibre volume fractions greater than about 10%, and that the fracture toughness of such composites, determined in the conventional fashion by tensile tests on double-edge-notched plates, was not a useful indicator of potential fatigue resistance. Furthermore, they found that resistance to fatigue failure in these materials was not a property that could be unambiguously defined, since it depended upon whether a constant stress range or constant strain range was adopted as the relevant design criterion. The experiments to be described in this paper are intended as a continuation of this earlier work: they attempt to show the effect of reinforcing with short fibres of various lengths, both uniaxially aligned and randomly distributed, on the resistance to crack propagation under monotonic and cyclic loading conditions in a composite system whose mechani-

cal characteristics are otherwise well known from the work of other investigators [2]. Another important reason for choosing to work with the Cu/W system instead of the Al-4%Cu/W system used by McGuire and Harris was to avoid the fibre/matrix interaction which these workers found to occur during hot-pressing, causing the formation of a brittle intermetallic layer at the interface which modified somewhat the process of crack initiation in the composites. We discuss here, therefore, the strength, fracture toughness and cyclic crack propagation resistance of copper/tungsten composites reinforced with chopped tungsten wires of various lengths which are either aligned in the direction of the applied stress or randomly distributed. These results are compared with others obtained on a number of samples reinforced with continuous fibres.

## 2. Experimental work

The samples used in this investigation were all manufactured by hot-pressing together in vacuum sheets of 99.9% pure copper and cold-drawn tungsten wires 0.38 mm in diameter. The short fibre composites were prepared by arranging chopped, cleaned wires of various lengths in grooves rolled or machined into the copper

\*Present address: NASA, Ames Research Center, Moffett Field, California, USA

sheets. These sheets were annealed, pickled and cleaned after grooving, and the wires arranged by hand in the grooves in such a way as to ensure random distribution of fibre ends. A dilute polystyrene/xylene binder was used to hold the wires in place while a stack of sheets was assembled and loaded into the press. This binder was burnt off during pre-heating and did not inhibit bonding across the fibre/matrix and matrix/matrix interfaces. The compacts were hot-pressed at 550°C at a pressure of about 45 MN m<sup>-2</sup> for 2 h during which time the vacuum usually remained better than 5 × 10<sup>-5</sup> torr. Continuous wire composites were prepared by threading 0.38 mm diameter wires through copper wire mesh (this being necessary to hold them straight and counter their natural tendency to curve after being removed from the reel) and interleaving the mesh between flat copper sheets prior to hot-pressing. A few randomly reinforced composites were also manufactured for comparison purposes by sprinkling a predetermined quantity of chopped wires onto copper sheets and again holding them in place with the binder while a stack was assembled for pressing. All short-wire composites contained approximately 25 vol% of fibres, but three different compositions of continuous composites were made. The latter could not be made with  $V_f$  as high as 0.25, however, because of the limitations of the manufacturing method. The compositions of all composites made are listed in Table I. The composite plates were about 70 mm × 70 mm and were pressed to a constant thickness of 3.5 mm.

Composite tensile properties were measured on parallel gauge section samples spark-cut

from the hot-pressed plates and ground to shape. The cross-section of the samples, which were 5 mm wide, was chosen so as to ensure that a reasonably large number of fibres was included, and a 25 mm gauge length extensometer was used to measure strains. All tests were carried out at an Instron cross head speed of 0.013 cm min<sup>-1</sup>. The strengths of the tungsten wire and the matrix copper were also determined.

Fracture experiments were carried out on 25 mm wide, double-edge-notched plates, using the same system as that described earlier [1]. The edge notches were spark-machined with a 0.127 mm diameter copper wire electrode to a depth of 6 mm, and crack-opening displacement gauges of the conventional type were used to plot load versus COD curves. The surfaces of samples were polished prior to testing so that crack growth and the development of plastic zones might be studied by means of a travelling microscope mounted on a rigid table in front of the Instron.

Cyclic crack propagation experiments were carried out in a servo-hydraulic fatigue machine on 50 mm wide, double-edge-notched plates containing spark cut notches 7.5 mm deep. These plates, which were also polished before testing, were subjected to fully-reversed, load-limited, tension/compression cycling at 15 Hz and crack-growth rates were determined by taking acetate film replicas of the central portion of the specimen at regular intervals without interrupting the test. Crack opening displacement measurements similar to those used to determine fracture toughness in monotonic loading were also made during cycling.

### 3. Experimental results

#### 3.1. Tensile properties

Stress/strain curves for the whole series of short-fibre composites are reproduced in Fig. 1, together with those for the unreinforced matrix and the tungsten wire. These show how composite strength increases with length of the reinforcing wires, and it can be seen that a species of "yield drop" occurs, the height of which also increases with fibre length. Immediately following this macroscopic yielding there is a flatter portion in the curves of most composites followed by a further rapid drop to a stress level well below the flow stress of the unreinforced matrix at equivalent strains. These curves may be compared with those of continuously reinforced

TABLE I Compositions of copper/tungsten composites used

Discontinuously reinforced; aligned		Discontinuously reinforced; random		Continuously reinforced; aligned
Fibre length mm	$V_f^*$	Fibre length mm	$V_f$	$V_f$
5	0.24	—	—	0.06
6	0.24	6	0.24	0.086
9.5	0.25	9.5	0.24	0.162
12.7	0.24	—	—	
17	0.25	17	0.22	
25.4	0.27	—	—	

\*Fibre volume fractions were determined gravimetrically.

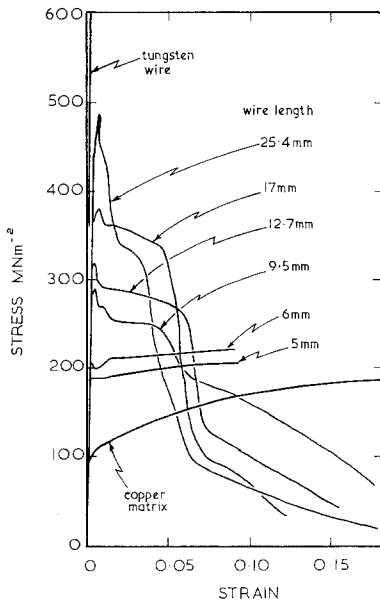


Figure 1 Stress/strain curves for aligned short-fibre copper/tungsten composites.

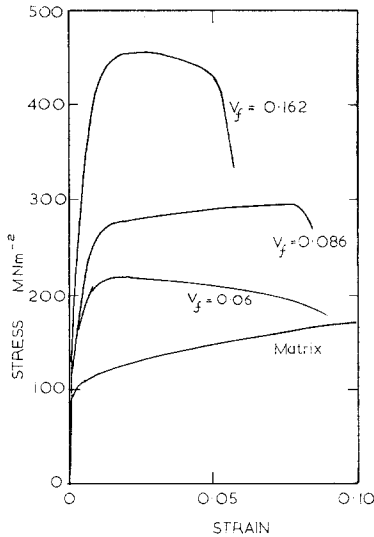


Figure 2 Stress/strain curves for continuous fibre composites.

composites and of randomly reinforced, short-fibre composites in Figs. 2 and 3. The continuously reinforced material behaves as expected but in the three random composites tested there was no strengthening. In Fig. 4, the ultimate and 0.2% yield stresses for continuous-fibre composites are plotted against fibre volume fraction together with values for the composites rein-

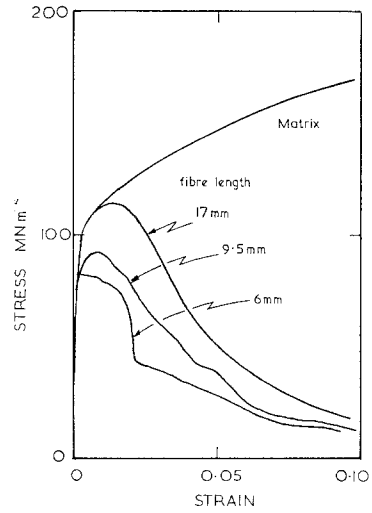


Figure 3 Stress/strain curves for random, short-fibre composites.

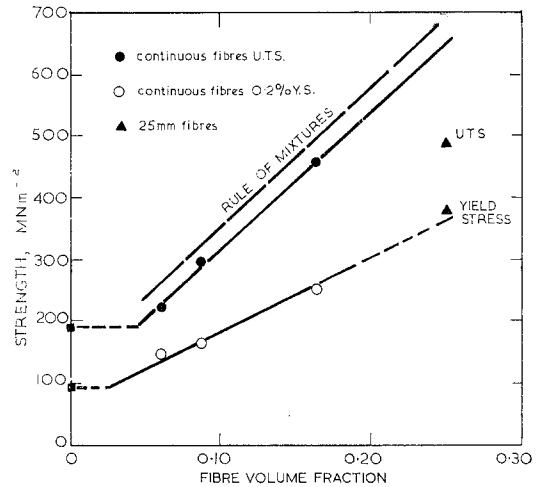


Figure 4 Ultimate tensile stress and 0.2% yield stress for continuous Cu/W composites, as a function of volume fraction, compared with values for the 25 mm short-fibre composites.

forced with aligned, 25 mm fibres. The experimental values of  $\sigma_c$  lie close to mixture rule predictions based on the measured fibre strength and the appropriate value of the matrix flow stress. The maximum stress of the 25 mm fibre composite is some 23% lower than the extrapolated value for continuous composites, but it can be seen that at yield the short fibres have as strong a reinforcing effect as continuous fibres, though they are little longer than the critical length.

If maximum stresses for the short-fibre composites are plotted as a function of aspect ratio,

$l/d$  (Fig. 5), the reinforcing effect is seen to be linear, as expected from elementary fibre reinforcement theory. Since it was clear from the appearance of tensile fractures that most of the wires used in this series of composites were shorter than  $l_c$ , the line in Fig. 5 represents the expression

$$\sigma_c = \tau(l/d) V_f + \sigma_{m,u}(1 - V_f), \quad l < l_c \quad (1)$$

where  $\tau$  is the fibre/matrix interfacial shear failure stress and  $\sigma_{m,u}$  is the matrix ultimate tensile

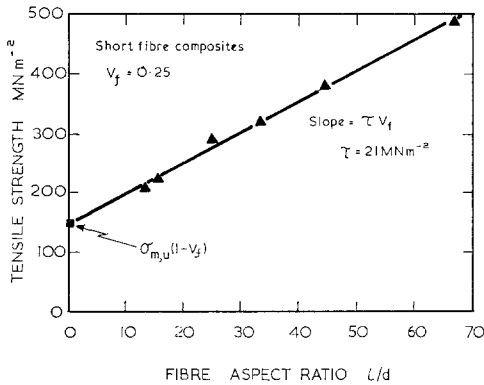


Figure 5 Tensile strength of short-fibre Cu/W composites as a function of fibre aspect ratio,  $l/d$ .

stress. The slope of the line is  $\tau V_f$  and the interface shear strength is therefore  $21 \text{ MN m}^{-2}$ . This relatively low value implies that bonding in these composites is poorer than is usual in cast composites of the same system. From the relationship

$$l_c/d = \sigma_f/2\tau$$

we find that the fibre critical length is 21.3 mm. The fact that this is just less than the length of the longest fibres used in these composites explain why the stress at yielding (prior to macroscopic plastic flow) in the 25 mm fibre composite is as high as would have been obtained in a continuous fibre composite of the same volume fraction, although the maximum stress, reached after the constraint has been removed by plastic deformation, is lower than that of the equivalent, continuous-fibre material.

The notched tensile strength,  $\sigma_N$ , of a number of samples was determined by machining small edge notches in the usual way into the centres of the gauge lengths of ordinary tensile test pieces. The results are given in Fig. 6 where the notched tensile stresses are plotted against the un-

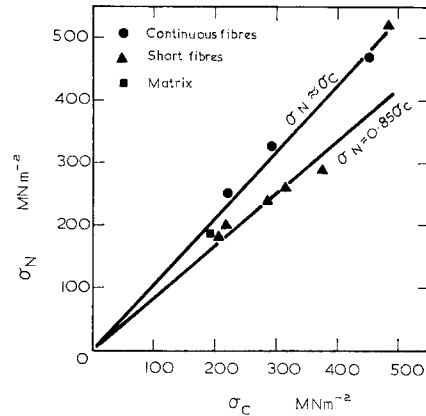


Figure 6 Notched and un-notched tensile strengths of continuous and short-fibre composites.

notched values. The strength ratio,  $\sigma_N/\sigma_c$ , for short-fibre composites with  $l < l_c$  is about 0.85, indicating some notch sensitivity, whereas for the composite containing 25 mm fibres and all continuous-fibre composites the ratio is close to unity. Similar insensitivity of the tensile strength to the presence of notches was found in Al-4%Cu/W composites by McGuire and Harris.

### 3.2. Fracture behaviour

In the curves of net section stress versus crack-opening displacement for short-fibre composites (Fig. 7) it can be seen that the effect of increasing the fibre length is small until the critical length is reached. Increases in both the peak stress and the area under the curve are far more significant once the fibre length exceeds  $l_c$ , and this behaviour is undoubtedly due to yielding and fracture of the 25 mm wires. This supports our

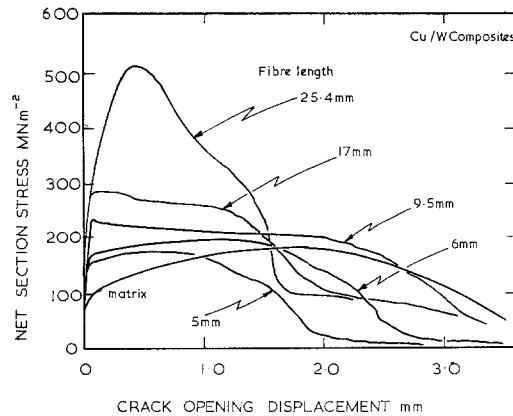


Figure 7 Crack-opening displacement curves for short-fibre Cu/W composites.

earlier premise that the 25 mm fibre composites may almost be treated as continuous-fibre composites in respect of their notch sensitivity and is further corroborated by a comparison of the curves in Fig. 7 with those for continuous composites in Fig. 8. Of the three randomly

fibre length in Fig. 9 where we see that their values are almost identical for fibre lengths up to 12 mm. There is an initial increase with fibre length up to about 10 mm followed by a plateau at a fracture energy of about 330 kJ m<sup>-2</sup>. The total fracture work remains at this level for

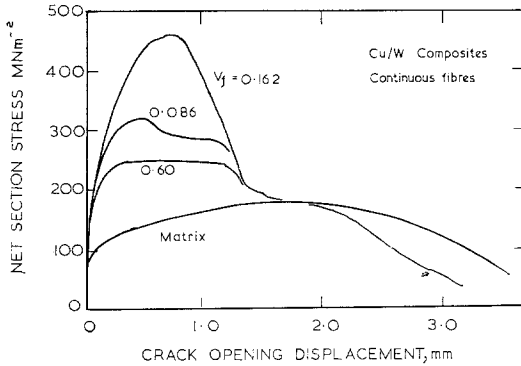


Figure 8 Crack-opening displacement curves for continuous-fibre composites.

reinforced composites, only those containing 17 mm wires reached the same peak stress as the unreinforced matrix, and the total energy to failure was drastically reduced in all cases.

From the COD experiments, the fracture work of the composites was obtained in two different ways. First, the entire stress/COD curve was integrated to obtain a work of fracture,  $\gamma_F$ , which is related to the total surface area of the two fracture faces. This total energy contains contributions from the work of fracture of the matrix and from the frictional work of fibre pull-out. In the case of continuous composites and those reinforced with 25 mm fibres, it also includes the work of deformation and fracture of the fibres themselves. It seems unlikely that for these composites there will be any significant debonding energy.

Secondly, a fracture energy was obtained from the relationship established by Wells [3] between crack extension force,  $G$ , and the critical value of the COD:

$$2\gamma_{COD} \approx G_c = (COD)_{crit} \cdot \sigma_y \quad (2)$$

where  $G_c$  is the crack tip fracture work and  $\sigma_y$  is the stress for plastic yielding which for these composites was taken as the secondary yield stress. This fracture parameter,  $\gamma_{COD}$ , refers to the critical condition only and may exclude the greater part of the pull-out work contained in  $\gamma_F$ . Values of  $\gamma_F$  and  $\gamma_{COD}$  are plotted against

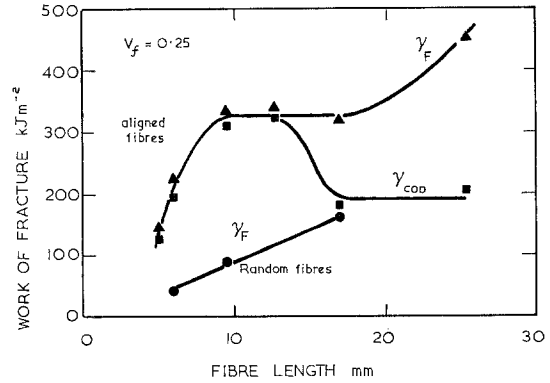


Figure 9 Work of fracture of short fibre Cu/W composites as a function of fibre length.

lengths up to about 17 mm whereafter it increases further as the effects of plastic yielding of the wire become more pronounced. For wire lengths greater than 12 mm, however, the value of  $\gamma_{COD}$  drops rapidly back to a level close to the mean value for the unreinforced matrix and shows no further increase even for fibres longer than  $l_c$ .

As a result of the relatively weak fibre/matrix bond, it was possible to see quite clearly during a COD experiment when the effort required to continue deforming the sample was being consumed exclusively in pulling out fibres. The total fracture energy,  $\gamma_F$ , could therefore be separated into two components for composites with fibres shorter than  $l_c$ :

$$\gamma_F = \gamma_P + \gamma_\mu$$

where  $\gamma_P$  is the work of plastically deforming the matrix and  $\gamma_\mu$  is the frictional pull-out work. By determining separately the areas under the stress/COD curves before and after the onset of the pull-out region it is possible to show the increasingly large contribution to the total fracture work from fibre pull-out. Cottrell [4] has shown that for fibres shorter than the critical length the frictional pull-out is given by

$$\gamma_\mu = \frac{V_f \tau l^2}{12d}, \quad l < l_c \quad (3)$$

Accordingly, the measured values of  $\gamma_\mu$  are

plotted in Fig. 10 as a function of  $l^2$ . From the slope of this curve we deduce that the interfacial friction stress is  $7.3 \text{ MN m}^{-2}$ , and extrapolating to the critical length, we find that the maximum possible value of pull-out energy is about  $180 \text{ kJ m}^{-2}$ . We note that this new value of the

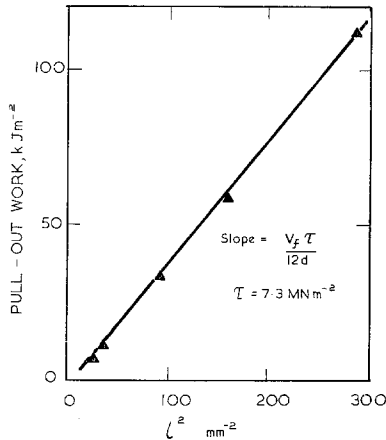


Figure 10 Frictional works of fracture, obtained by integration of those parts of the COD curves in Fig. 7 that relate principally to fibre pull-out, as a function of (fibre length)<sup>2</sup>.

interfacial shear stress is only about a third of the value obtained from tensile strength measurements.

The works of fracture for continuously reinforced composites are plotted against  $V_f$  in Fig. 11. The variations between  $\gamma_F$  and  $\gamma_{\text{COD}}$

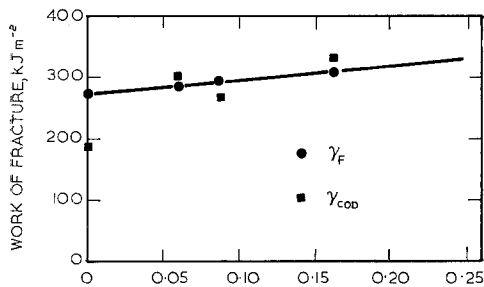


Figure 11 Work of fracture for continuous fibre composites as a function of fibre volume fraction.

are small by normal standards of fracture toughness testing, but the values of total fracture energy give the clearer picture of composite behaviour. The fracture work increases linearly with increasing volume fraction, but the overall effect of as

much as 16% of wire is quite small, which implies that it is the matrix which largely determines the fracture behaviour of the composites. Observations of fracture surfaces showed that pull-out lengths of broken fibres were small and of the same order of magnitude as those in the discontinuous composites containing the shortest fibres. It would seem, therefore, that the pull-out energy in the continuous-fibre samples is insignificant and that the increase in composite toughness is due only to the addition of the fibre fracture energy to that of the matrix, the two contributing in proportion to their respective volume fractions. On the other hand, since the shorter fibres in the discontinuously reinforced composites are too short to be plastically deformed or broken, the composite gains a small amount of pull-out energy but loses matrix fracture work in proportion to the volume fraction of non-deforming wires. The fracture energy of continuous composites (extrapolated to 25 vol %) is identical with that of the short fibre composites reinforced with 12 and 17 mm long wires.

The fracture work of randomly reinforced composites was disappointingly low, as shown in the lower part of Fig. 9. There seems little reason to suppose that the matrix contribution should be diminished and every reason to suppose that, although no *tensile* deformation of fibres would occur, there would at least be a substantial contribution from plastic bending of those wires which are not aligned with the specimen testing direction and must therefore be bent straight in order for the composite to be broken into two pieces [5]. This expectation is clearly not upheld, however.

### 3.3. Crack propagation under cyclic loading

The intention in this part of the experimental program had been to study the rate of crack propagation ( $dc/dN$ ) during cyclic loading as a function of the applied stress intensity range,  $\Delta K$ , in order to deduce a single design parameter that could characterize differences in material behaviour between unreinforced matrix, continuous fibre composites and chopped wire composites. Unfortunately we were unable to complete the program in the manner envisaged because substantial differences in fracture behaviour made it impossible to apply a single analysis to all three materials. In the matrix and in the 6% and 8.6% continuous-fibre composites, stable crack

growth occurred. In the 16.2% composite, however, cracks could not propagate because splitting occurred at notch roots with consequent blunting of the notches. Furthermore, since the composites are so much stronger than the unreinforced matrix, the stresses needed to cause stable crack growth in composites were too high for the plain copper so that direct comparisons could not be made. Finally, cracks could not be made to propagate in the short-fibre composites under any circumstances except over very short distances at the start of a test. There was thus no possibility of obtaining a quantitative assessment of resistance to crack growth under cyclic loading conditions.

Fig. 12 shows some typical crack growth curves for the matrix copper and for two

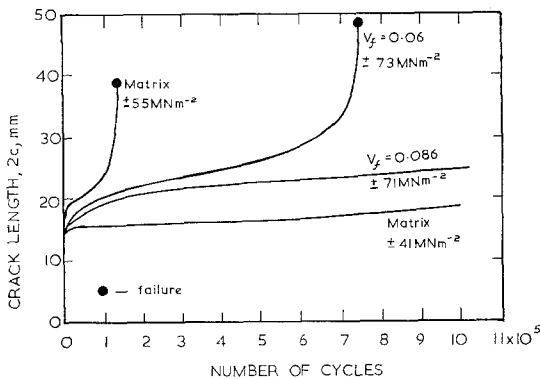


Figure 12 Typical crack growth curves for the copper matrix and two continuous-fibre composites at various stresses. The crack length is given as  $2c$  because these are double-edge notched samples.

continuous-fibre composites. The stress range represented for the unreinforced matrix is  $\pm 41 \text{ MN m}^{-2}$  to  $\pm 55 \text{ MN m}^{-2}$ , and at these limits the material shows either long life with stabilization of the crack by plastic zone formation, or rapid propagation to failure in a few thousand cycles. The two composite curves are for stresses about the level of the normal yield stress of the plain matrix and the curves show the strong crack retarding effect resulting from the presence of continuous fibres. Observation of composite fracture surfaces showed that the shapes of crack-growth curves were related to the mode of failure of the wires. In early and intermediate stages of growth (up to 50-60% of sample life) the wire fractures had a “shattered” appearance and were extensively fragmented.

Beyond this point, during the second stage of growth, the wire fractures were of a brittle cleavage type with a granular appearance, and in the concluding stage the wires failed by necking in a conventional tensile mode. For the most part, then, it seems that the rate of stable crack growth is controlled by fibre fatigue arising from build-up of crack tip stresses as a result of local matrix work hardening. Only in the later stages of growth do the crack tip stresses become sufficiently large to initiate brittle failure with a concomitant rapid increase in growth rate and the final, ductile failure occurs when too few wires remain to support the stress applied to the composite.

Stable crack growth could not be induced in any of the short-fibre composites even when, after some blunting of the initial notches had occurred, the test was stopped and the notches resharpener. It appeared to be possible to cycle all of these composites almost indefinitely at stress intensity ranges high enough to induce stable crack growth and brittle failure of the unreinforced matrix after only  $10^5$  cycles. The curves in Fig. 13 are typical of the crack growth

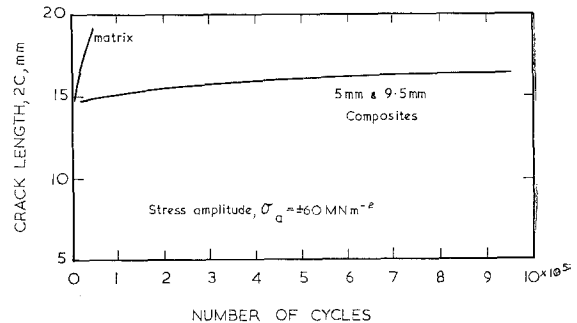


Figure 13 Crack growth curves for 5 mm and 9.5 mm short-fibre composites and the copper matrix at a stress amplitude of  $\pm 60 \text{ MN m}^{-2}$ .

behaviour in these materials. Initial notches were soon blunted and instead of the localized plastic strain that accompanies crack propagation in continuous-fibre composites smaller amounts of uniformly distributed plastic deformation occurred throughout the sample. Small holes frequently appeared at the ends of wires. At higher stress intensities failure occurred by a process of step-wise, interfacial crack propagation in which interfaces parallel to the stress axis gradually opened up and were finally linked by small, transverse cracks. This behaviour appears

to be a result of the weak interface and the high volume fraction which together encourage splitting; this also occurred in the 16% continuous-fibre composites. It is interesting to note that whereas some significant change in fatigue failure mode had been expected in composites containing fibres longer than  $l_c$ , no such change was observed. Post-fatigue tensile and COD tests were carried out on some of the short-fibre composites and it was found that although the strength was usually unaffected by fatigue damage, the fracture energy was significantly reduced, clearly as a result of the reduction in the matrix contribution to fracture work.

#### 4. Discussion

Kelly and Lilholt [6] and others have shown that in systems where the ultimate stress of composites can be accurately represented by the rule of mixtures relationship, there are frequently deviations from the rule at low strains. By extrapolating back from the fibre and composite strengths it is found that the flow stress curve for the matrix *in the composite* is different from the curve for the unreinforced matrix, rising well above it but falling back to meet it by the time the composite maximum stress is reached. This has been ascribed by Kelly and Lilholt to effects of constraint arising from Poisson's ratio differences, and such a constraint would naturally be expected to disappear when both fibre and matrix were deforming plastically. The fact that yield drops occur in the stress/strain curves of Fig. 1 suggests that similar effects are occurring in our composites and that these drops are associated with sudden loss of constraint. Derived matrix stress/strain curves [7] do indeed show very large positive deviations from the plain matrix curves determined in separate tensile tests. Instances have been found where the flow stress of the matrix in the composite is twice that of the unreinforced matrix at the same strain. The value of the interfacial shear strength ( $21 \text{ MN m}^{-2}$ ) derived from these data corresponds to the maximum stress levels of the stress/strain curves and therefore to the point at which the constraint is a maximum. We have seen, however, that this level of shear stress is not maintained in tests where cracks are propagating through the composite and fibres are pulling out against an

interfacial friction only a third of the value for the constrained state.\*

If the data of Figs. 9 and 11 are replotted against reciprocal fibre length it is possible to obtain a direct comparison between the toughness of continuous and short-fibre composites that suggests a suitable interpretation. In Fig. 14a

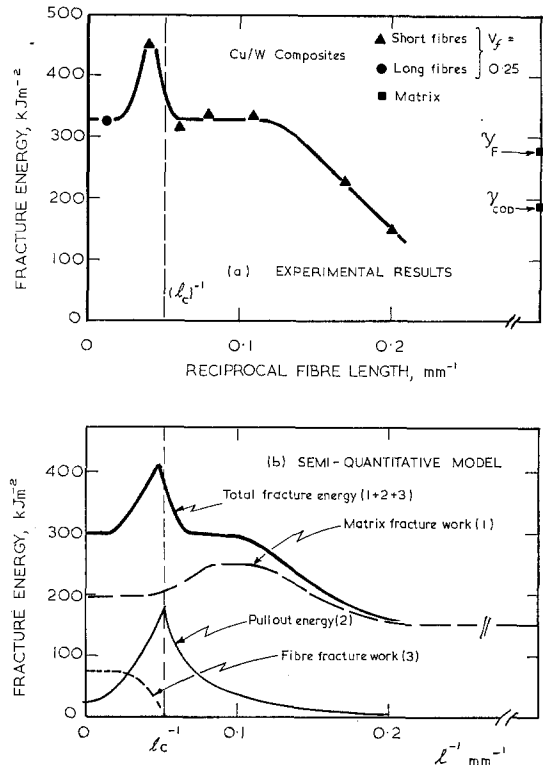


Figure 14 Fracture energy of Cu/W composites as a function of reciprocal fibre length, showing (a) experimental results and (b) a semi-quantitative model to illustrate how the form of the experimental curve could be obtained by summing separate contributions to the total fracture energy.

we see that the fracture energy value at the shortest fibre lengths rises with increasing  $l$  until it reaches a plateau at about 9.5 mm which continues, apart from a single excursion, to continuous-fibre composites of length 80 mm (as used in these experiments) and, by logical extension, to infinitely long samples for  $l^{-1} = 0$ . This curve begins below the lowest level of toughness obtained for the unreinforced matrix

\*Since this manuscript was prepared, R. E. Lee and S. J. Harris (*J. Mater. Sci.* 9 (1974) 359) have published some results on matrix strengthening in continuous-fibre Cu/W composites. They used tungsten wires at least an order of magnitude smaller in diameter than ours, and their results would seem to imply that no anomalous matrix strengthening should have been observed with wires as thick as ours were.



( $\gamma_{\text{COD}}$ ) and finishes at a level only slightly above that of the highest value ( $\gamma_F$ ). It seems reasonable to assert, therefore, that the fracture work of these composites is largely derived from the work of plastic deformation of the matrix, and that the relatively small variations observed with changes in fibre length are mostly due to modification by the fibres of the matrix plastic flow characteristics. The single point which stands off the basic curve falls, significantly, close to the critical length, and is not a freak result. An explanatory model for these results calls for a consideration of the separate effects that might contribute to the work of fracture of the composite. We now suppose that the total fracture work,  $\gamma_F$ , can be broken down in the following manner:

$$\gamma_F = \gamma_M(l) + \gamma_f + \gamma_\mu$$

where  $\gamma_M(l)$  is a variable matrix work of fracture and  $\gamma_f$  is the fibre work of fracture. We have already discussed  $\gamma_\mu$  and we know that it is proportional to  $l^2$  increasing to a maximum value of about  $180 \text{ kJ m}^{-2}$  at  $l_c$ . If the fibres are longer than  $l_c$ , a proportion  $l_c/l$  only will be able to pull out and contribute to  $\gamma_\mu$ . For continuous-fibre composites the amount of pull-out is not zero, however, as the original suggestion of Kelly [8] would imply, and our observations suggest that it remains at about the same level as that observed in 6 mm fibre composites. Since this defines a limit to pull-out work for  $l > l_c$ , the variation of  $\gamma_\mu$  can be plotted on the semi-schematic diagram of Fig. 14b. Those fibres longer than  $l_c$  which do not pull out, a proportion  $(1 - l_c/l)$ , must contribute their own plastic work of fracture. This is not easy to determine, for it involves a knowledge of the deforming volume as well as the stress/strain curve, but integrating our own measured stress/strain curve for the tungsten wire gives a work per unit volume of about  $40 \text{ MJ m}^{-3}$  per fibre. Inspection of fracture surfaces revealed that only about 53% of the wires failed in a ductile manner, the rest failing with no sign of plastic flow, and that in the ductile fibres the deformation was limited to a region about 1 mm long on either side of the fracture face. For a volume fraction of 0.25, then, the maximum value of plastic work of fracture that can be attributed to the fibres is about  $80 \text{ kJ m}^{-2}$  and this builds up in a roughly logarithmic fashion, as shown in Fig. 14b, after the fibre length exceeds  $l_c$ . The increase in  $\gamma_f$  thus compensates to some extent for the fall in pull-out work when fibres begin to

break. The cause of the peak in Fig. 14a may now be perceived, and it remains to deduce how  $\gamma_M(l)$  varies with fibre length in order to raise the overall level of the hypothetical work curve to the level of the experimental results. It is not sufficient, however, to assume that a constant proportion of the matrix fracture work,  $\gamma_F(1 - V_f)$ , should be added. The work of fracture of the plain matrix,  $\gamma_F$ , is  $272 \text{ kJ m}^{-2}$ , whereas that determined from the critical COD value was only  $178 \text{ kJ m}^{-2}$ . It seems likely that the principal difference between the conditions of the two tests is that the  $\gamma_F$  value involves a somewhat higher volume of plastically deforming copper than  $\gamma_{\text{COD}}$ . An alternative way of looking at it might be that the lower value of the fracture energy would be more appropriate for a situation involving a higher degree of constraint—a plane strain, as opposed to a plane stress situation, for example. As we saw earlier, it is likely that the copper containing 25% of tungsten wires is subject to a high degree of constraint, and it seems appropriate to start the matrix contribution to the composite  $\gamma_F$  at a value of 75%, or  $(1 - V_f)$ , of the value of  $\gamma_{\text{COD}}$ . As cracks propagate in the short-fibre composites, they are deflected to an extent that will depend on the fibre length, and as the fibre length is increased, therefore, more of the matrix material is forced to deform plastically. Observations of surface appearance confirm that the size of the plastic zone increased with increasing fibre length, but beyond the 9 mm fibre point there appeared to be little further increase in the plastically deforming volume. On the other hand, we have seen that the degree of matrix strengthening and concomitant constraint also increases with increasing fibre length, and the rate of increase is greater at the longer fibre lengths. The net result is that the matrix fracture work,  $\gamma_M(l)$ , must fall with increasing fibre length after having first increased as the volume of deforming material increased. The fact that these two processes are not quite in phase means that the curve for the matrix contribution must now show a hump as shown in Fig. 14b. There seems no easy way of deducing the exact shape and level of this curve, and its representation is therefore schematic. However it varies only between the limits of fracture work for the unreinforced matrix previously discussed. Summation of the three constituent curves then gives a total work of fracture curve of the same general form as the experimental one and the

semi-quantitative agreement between the two is reasonably satisfactory.

Assessment of the fatigue crack propagation results in terms of a single design parameter is out of the question, as we have seen, because of the extremely high resistance to crack growth in short-fibre composites resulting from delocalization of plastic strain. This high apparent resistance to crack growth is independent of fibre length and is presumably due to the relatively weak interface. This facilitates splitting and therefore prevents dangerous build up of stresses at crack tips which, in continuously reinforced composites, leads to fibre fatigue failures. Baker [9] has carried out fatigue experiments on aluminium reinforced with chopped steel wires of various lengths. In this system there is interaction between fibres and matrix and the interfacial bond is good. Baker found that increasing the fibre length from 6 to 25 mm substantially improved the low cycle fatigue resistance and that his short-fibre composites failed in the same manner as continuously reinforced materials. On the other hand he showed that for a given plastic strain range, his composites containing continuous fibres performed somewhat better than short-fibre composites reinforced with 13 mm fibres but less well than those containing 25 mm fibres. Furthermore, he showed two regimes of behaviour. At low plastic strain levels the fatigue life was determined by matrix and interface damage caused by fine cracks that could not penetrate

the fibres, and the fatigue lives of composites were much higher than those of the unreinforced matrix at similar plastic strain ranges. At high levels of plastic strain, however, the efficiency of reinforcement was substantially reduced and the fatigue lives were close to those expected of the unreinforced matrix because the fibres could no longer prevent direct crack propagation. Only at low strain levels, therefore, were the properties of short-fibre composites inferior to those reinforced with continuous fibres. The difference between our results and Baker's can presumably be explained in terms of the relative interfacial strengths.

A number of attempts have been made to apply fracture mechanics ideas to fatigue crack propagation in homogeneous materials [10], and Gerberich [11] has developed a model which extends the approach to composite materials. These theories all result in a fourth power correlation between rate of crack growth with number of cycles,  $(dc/dN)$ , and the stress intensity range,  $\Delta K$ , of the form

$$dc/dN \propto (\Delta K)^4$$

and in practice most experimental results do appear to confirm this fourth power dependence. Gerberich applied his model to the behaviour of a 2024 aluminium alloy reinforced with continuous stainless steel fibres and showed that the fourth power dependence was equally valid for the matrix alloy and for composites with up to 20 vol % of fibres. Our own results for continu-

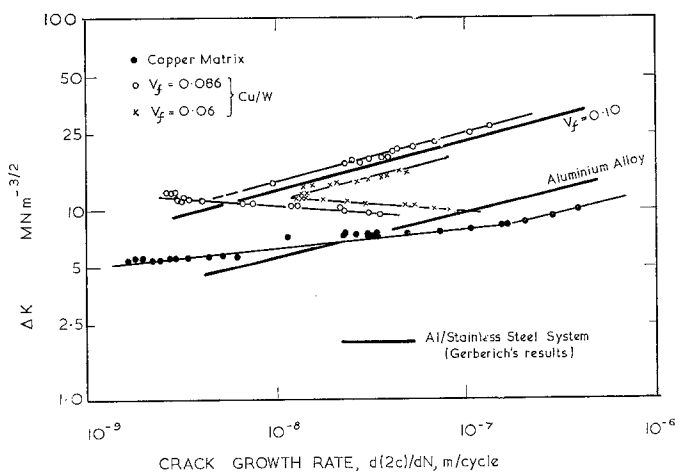


Figure 15 Stress intensity range,  $\Delta K$ , versus crack growth rate for copper/tungsten composites reinforced with continuous fibres. These curves are compared with results for the unreinforced matrix and for a 10 vol % aluminium alloy/stainless steel composite [11].

ous composites are plotted in terms of the crack growth rate  $d(2c)/dN$  as a function of stress intensity range,  $\Delta K$ , in Fig. 15. Calculation of  $\Delta K$  was carried out by means of an iteration program based on the standard Srawley and Brown expression [12] and the plastic zone correction factor for crack length,  $c = c_0 + w$ , where  $c_0$  is the measured length and  $w = \frac{1}{2}(\Delta K/2\sigma_y)^2$ . The factor  $\frac{1}{2}$  accounts for the suggestion that it is only the tensile part of the cycle that influences crack growth. And whereas this, and indeed the whole question of applying standard expressions to anisotropic, inhomogeneous composites, may be called into question by purists, the results nevertheless give an interesting comparison with Gerberich's own work. Fig. 15 shows that the  $\log \Delta K/\log$  (growth rate) curves for the matrix, and for the 6% and 8.6% composites are linear; and although the matrix curve is much flatter than the predicted fourth power relationship at low growth rates, it is beginning to develop a  $\frac{1}{4}$  slope above rates of about  $10^{-7}$  m cycle $^{-1}$ . The higher branches of the composite curves show an approximate fourth-power dependence, and the general performance of matrix and composites may be compared with two of Gerberich's curves, one for the matrix aluminium alloy and one for a 10 vol % composite, which are also shown. The data for Gerberich's composites may best be compared with ours by cross-plotting the stress intensity range for a constant growth rate of  $10^{-7}$  m cycle $^{-1}$  against volume fraction as shown in Fig. 16. The similarity of the results is quite striking, but over the limited range of com-

positions covered it appears that the rate of improvement in the Cu/W system with  $V_f$  is greater than that in the Al/steel composites. This would surely be due to the higher strength and fatigue resistance of the tungsten fibres and the weaker interface.

One curiosity in Fig. 15 is that the composite curves are double branched and at  $\Delta K$  values below  $10 \text{ MN m}^{-3/2}$  they show negative slopes. This implies a mechanistic change below this level. It suggests that in the low stress range the wires have a crack retarding effect sufficiently strong to change completely the character of the fatigue process. But in the high stress range the wires offer little direct resistance to crack growth as already discussed in relation to the observed brittle fracture of wires in later stages of growth, in which region the values of the power law exponent are similar to those observed for normal metals. These observations are admittedly for very different conditions from those used in Baker's work, but the implications are identical.

### Acknowledgements

The authors wish to record their thanks to the Ministry of Defence, Procurement Executive, for generous financial support during the execution of this programme, and it is with their permission that these results are published.

### References

1. M. A. MCGUIRE and B. HARRIS, *J. Physics D*, **7** (1974) 1788.
2. G. A. COOPER and A. KELLY, *J. Mech. Phys. Solids* **15** (1967) 279.
3. A. A. WELLS, Proc. Cranfield Crack Propagation Symposium, 1962.
4. A. H. COTTRELL, *Proc. Roy. Soc. A* **282** (1963) 1.
5. J. HELFET and B. HARRIS, *J. Mater. Sci.* **7** (1972) 494.
6. A. KELLY and H. LILHOLT, *Phil. Mag.* **20** (1969) 311.
7. S. V. RAMANI, D.Phil. thesis, (1974) University of Sussex.
8. A. KELLY, "Strong Solids", (Clarendon Press, 1966 (1st edn.)).
9. A. A. BAKER, *Applied Matls. Research* (October 1966) 210.
10. J. R. RICE, ASTM, Special Technical Publication no. 415 (1966) 247.
11. W. W. GERBERICH, Ph.D. thesis, University of California (L.R.L.), 1971. Also issued as report UCRL-20524, Feb. 1971.
12. W. F. BROWN and J. E. SRAWLEY, ASTM Special Technical Publication no. 410 (1966) 11.

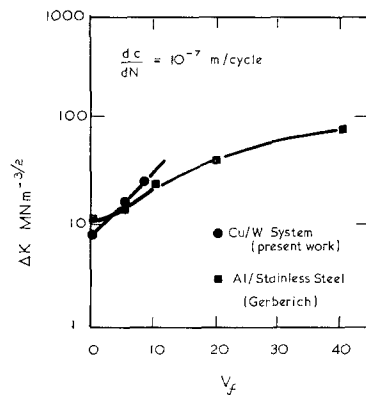


Figure 16 Comparison of the stress intensity range for a crack growth rate of  $10^{-7}$  m cycle $^{-1}$  as a function of fibre volume fraction for the Cu/W system and for the Al/steel system of Gerberich [11].

Received 24 June and accepted 15 July 1974